International Journal of Thin Films Science and Technology

http://dx.doi.org/10.12785/ijtfst/030104

Study of Structural, Morphological and Optical Properties of Sb_2S_3 Thin Films Deposited by Oblique Angle Deposition

*A. Sinaoui**, *I. Trabelsi, F. Chaffar Akkar, F. Aousgi and M. Kanzari*

Laboratoire de Photovoltaïques et Matériaux de Semi-conducteurs-ENIT-Université de Tunis el Manar, BP 37, le belvédère1002-Tunis, Tunisie

Received: 7 Jun. 2013, Revised: 21 Sep. 2013, Accepted: 23 Sep. 2013
Published online: 1 Jan. 2014

Abstract: Sb_2S_3 thin films were deposited by thermal evaporation method with oblique angle deposition technique. During the deposition, the substrate temperature was maintained at T_s = 180 °*C* and the deposition angle was fixed at $\alpha = 0°$, 20°, 40°, 60°, 70° and 85°. X-Ray Diffraction (XRD), Atomic Force Microscopy (AFM) and UV- Vis- NIR spectra were used to characterize the structural, surface morphology and optical properties respectively of the layers. X-ray diffraction spectra indicated that all the deposited Sb_2S_3 films are amorphous. The band gaps of the thin films were found to be direct allowed transitions and are around 1.87 eV. In addition it was found that the refractive index decreases from 2.98 for $\alpha = 0°$ to 2.28 for $\alpha = 85°$. The relationship between the flux incident angle α and the column angle β was also explored.

Keywords: Sb_2S_3 thin films, Oblique angle deposition, Structural properties, Optical properties.

1 Introduction

The oblique angle deposition (OAD) technique has attracted a lot of attention in many different applications due to their unique advantages of programmable nanomorphologies [1,2]. It is a useful method to deposit variable microstructure films which is hardly obtained by the normal incidence deposition [3]. It is based on thin films deposition by physical vapor deposition and employs oblique angle deposition [1,2]. Therefore OAD technique have high porosity and anisotropic behavior [4, 5]. The oblique angle flux incidence enhances atomic shadowing and creates inclined columns microstructures. It has been accepted that the columns obtained from this deposition are oblique, but due to the shadowing effect, the column angle β measured to the substrate normal is smaller than the angle between the flux of the particles and substrate normal [8].

There are several actual and potential technological applications of chalcogenide materials due to the possibility of modifying their physical properties such as optical band gap and index of refraction [9]. Antimony Sulphide is a chalcogenide semiconductor which crystallizes in the orthorhombic structure (Pbnm) with cell parameters, a = 11.2 *Å*, b = 11.32 *Å* and c = 3.84 *Å* at room temperature [10]. Due to its attractive photo conducting properties and high thermoelectric power, Sb_2S_3 has wide industrial applications such as target material in television camera, microwave devices, switching devices and optoelectronic devices [11]. Chalcogenide materials can be fabricated in amorphous form in several ways, including the OAD technique [7].

In this paper, we present a study describing the effect of oblique angle deposition on the structural, morphological and optical properties of Sb_2S_3 thin films.

2 Experimental Work

2.1 Synthesis of Sb_2S_3 crystal

Stoichiometric amounts of the elements of 99.999 % purity antimony Sb and sulphur S were used to prepare the initial ingot of the Sb_2S_3 material. The mixture was sealed in vacuum in a quartz tube. In order to avoid explosions due to sulfur vapor presses, the quartz tube was heated slowly (20 °*C*/h). A complete homogenization

* Corresponding author e-mail: azzasinaoui@yahoo.fr

could be obtained by keeping the melt at 650 $^{\circ}C$ for 48 h. The tube was then cooled at the rate 7 $^{\circ}C$/h. Therefore cracking, due to thermal expansion of the melt on solidification, was avoided. The compound obtained is dark grayish color. X-ray diffraction of Sb_2S_3 powder analysis showed that only the Sb_2S_3 phase was present in the ingot (Fig.**1**).

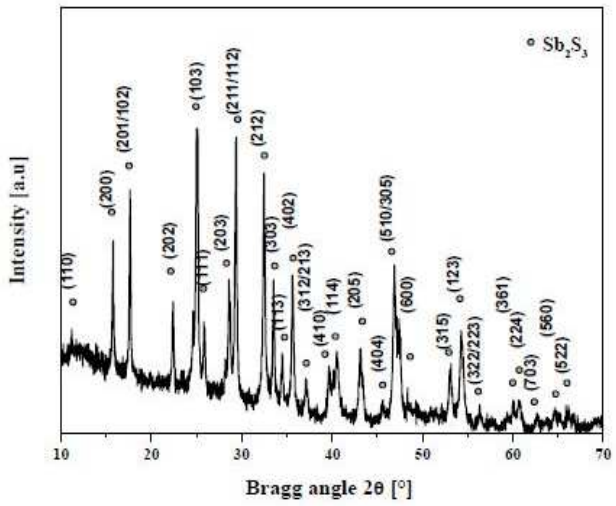

Fig. 1: The X-ray diffraction patterns of the Sb_2S_3 powder.

2.2 Film preparation

Sb_2S_3 thin films were prepared by thermal evaporation from a Tungsten boat on glass substrates heated at 180 $^{\circ}C$ using a high vacuum coating unit Alcatel. All the films were deposited onto heated glass substrates of rectangular shape (2.5 $\times$ 1.5 cm^2) using the OAD technique. The substrates were placed directly above the source at a distance of 10 cm and were heated by an halogen lamp. During our experiments, the angle between the surface normal of the target and the surface normal of the substrate was fixed at α = 0°, 20°, 40°, 60°, 70° and 85°. The substrate temperature Ts was measured using a thermocouple embedded in the substrate holder underneath the substrates. The glass substrates were previously cleaned with washing agents (commercial detergent, acetone, ethanol and deionized water) before being introduced into the vacuum system.

3 Characterization of the Sb_2S_3 thin films

The crystalline phase and crystal orientation of the powders and the films were examined using a Philips X'Pert X-ray diffractometer with monochromatic CuKα radiation (λ = 0.154056 nm). The surface morphology of the films was characterized successively by atomic force microscopy (Veeco Dimension 3100 AFM). The transmittance and reflectance spectra of the OAD films were measured with an UV visibleNIR Shimadzu 3100 S spectrophotometer in the spectral range 300 - 1800 nm.

4 Results and Discussions

4.1 Structural properties

Figure **1** shows the X-ray diffraction patterns (XRD) of the synthesized powder of the Sb_2S_3 material. It is clear that, the sharp peaks present in the pattern indicate the polycrystalline nature of the sample and confirms that only the Sb_2S_3 phase is present with the preferential orientation following the plane (103) [12].

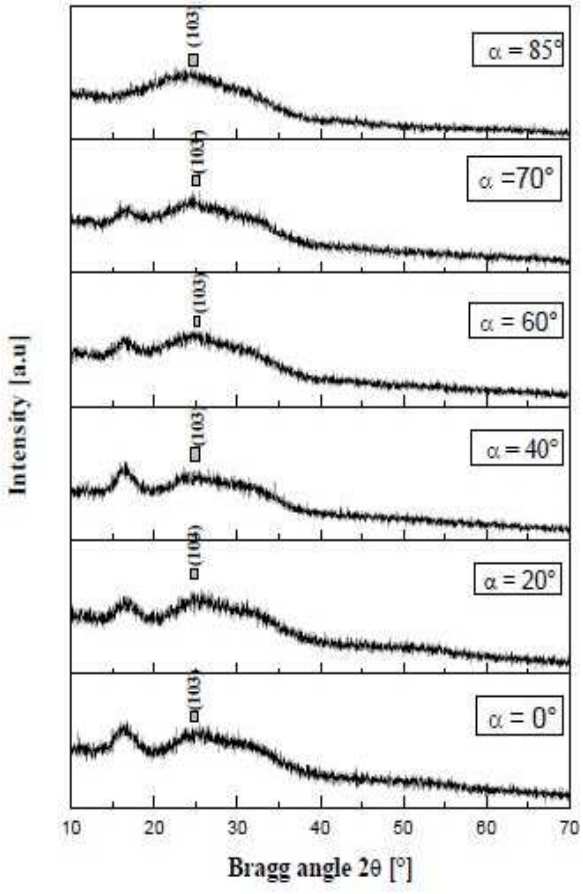

Fig. 2: The X-ray diffraction patterns of the Sb_2S_3 films deposited, respectively, at different incident angles.

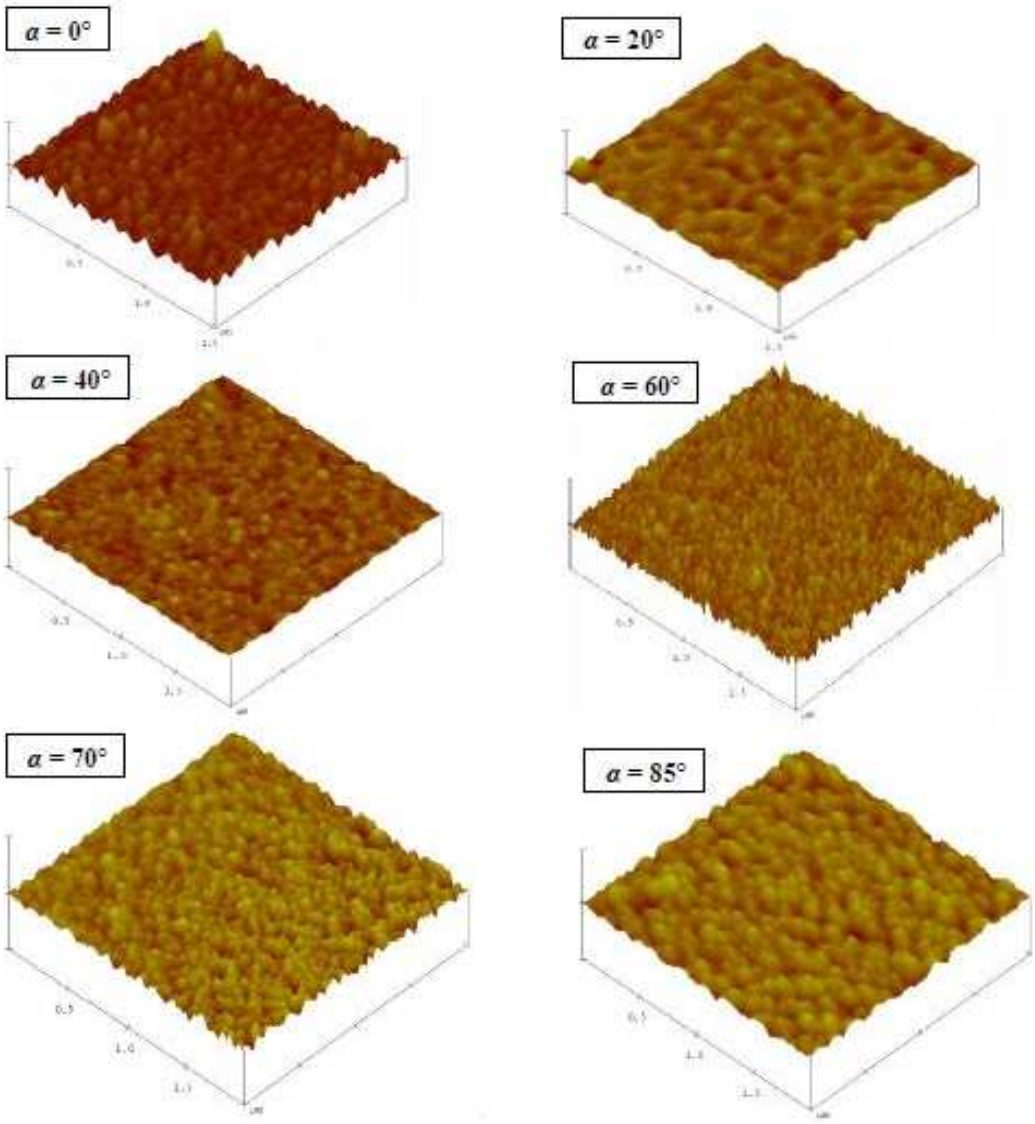

Fig. 3: AFM images of surfaces of Sb_2S_3 films deposited, respectively, at diffrent incident angles.

Figure **2** shows the X-Ray diffraction patterns of the Sb_2S_3 thin films deposited respectively at α = 0°, 20°, 40°, 60°, 70° and 85°. As can be seen, the peaks are broadened and their lower intensity suggests poorer structural quality, thus, the XRD analysis of the all deposited Sb_2S_3 thin films, revealed that all the investigated films formed at T_s = 180 °C have an amorphous nature, which agrees with the previous observations reported by [12]. The obtained results confirmed that OAD technique cannot influence much in the amorphous nature of all the films. With increasing the substrate temperature ($T_s \geq$ 400 °C), the surface diffusion of the adsorbed species becomes higher resulting in an improvement in the quality and crytallinity of the films. Indeed, grain boundary migration and recrystallization are possible [13].

4.2 Morphological properties

The surface morphologies of the OAD Sb_2S_3 thin films are presented by AFM images shown in figure **3**. From these images, it is clear that the surface topography changed when the incidence angle of the atoms was different from 0°. Indeed, for the flux angle as 0°, the picture shows smooth and homogenous surface constituted of densely packed grains and when the flux incident angle increases, the surfaces become rougher and

porous due to poor crystallinity, which was also confirmed by X-Ray diffraction data.

We note also that, for the flux angle as 0°, the column's top are randomly orientated, whereas, for the film deposited at α = 85°, the film is constituted of rounded grains which are tilted toward the incident deposition flux. Indeed, at high incident angle, the surface of the film shows a columnar structure consisting of slanted thin columns with a great deal of pores in the neighboring columns. Thus, we can say that the morphological properties of OAD technique are enhanced by shadowing effect and limited by the surface diffusion of adatoms during the film growth. The shadowing effect which dominates the growth process produces porous and low density thin films [14]

The columnar structure is a result of the shadowing effect. In general, the column angle β, which is defined as the angle between substrate normal and the long axis of slanted columns, is less than the vapor incident angle α and follows the tangent rule for small α ($\alpha \leq 50°$) [5,6]:

$$\tan\beta = \frac{1}{2}\tan\alpha \quad (1)$$

or the cosine rule for higher α ($\alpha > 50°$) [7]:

$$\beta = \alpha - \arcsin\left(\frac{1-\cos\alpha}{2}\right) \quad (2)$$

The measured column angle β at α = 85° is 39 which is rather lower than the theoretical prediction of β = 57° calculated by the cosine rule. The origin of this deviation may be due to the difference of material, deposition parameters (deposition pressure and temperature) and flux vapor angular distribution. The surface roughness of Sb_2S_3 thin films deposited at different incident angles was determined from AFM pictures and the root-mean-square (RMS) roughness values are listed in Table **1**. It was observed that the surface roughness of the films increases with increasing the deposition angle α and the films became rougher when the deposition angle increases which can be linked to the porosity of the films. One can suggest that a high flux angle favors a much more porous structure. For example, the surface roughness of Sb_2S_3 films deposited at α = 0° and α = 85° increases from 2.12 nm to 9.36 nm, respectively. This property is important because rougher surfaces can advance optical scattering [15] and can increase the effective area for advanced charge storage devices [16]. These properties of thin films are exploited in a number of applications, including semiconductor devices and solar cells [17].

4.3 Optical properties

The transmittance and reflectance spectra of Sb_2S_3 thin films deposited at different flux incident angles in a wavelength range of 300 1800 nm, grown on substrates heated at 180 °C are shown in figure **4**.

The transmission and the reflection spectra's show interference patterns with sharp fall of the transmission at the band edge, which is an indication of good homogeneity of the films, whereas the interference effects disappear for higher incident angle, especially at α = 85° which can be explained by the shadowing effect and limited adatom diffusion which inhibits the diffusivity of deposited atoms [18].

The average of the transmission and the reflection of all the layers in the transparency region (700 - 1800 nm) are about 65% and 35% respectively. We note also from the transmittance spectra, that the absorption edge was displaced to the low wavelengths as the deposition angle α increases and there is no transmission for the low wavelength because all the light is absorbed.

Based on the reflectance spectra of the Sb_2S_3 thin films, the thickness and the refractive index of the different films deposited respectively at α = 0°, 20°, 40°, 60°, 70° and 85° were calculated from the positions of the interference maxima and minima of reflectance using a standard method [19]. The values of the refractive index and the thickness of the Sb_2S_3 films are shown in Table **1**.

It is clear from this table, that the refractive index of Sb_2S_3 thin films decreases with the increase of deposition angle from 2.98 at α = 0° to 2.28 at α = 85° which can be explained by the decrease of the thickness of the samples as the deposition angle a increases. The effective packing density of OAD Sb_2S_3 films can be calculated using Bruggeman effective medium approximation [20]:

$$P_A\frac{\varepsilon_A-\varepsilon}{\varepsilon_A+2\varepsilon}+P_B\frac{\varepsilon_B-\varepsilon}{\varepsilon_B+2\varepsilon} \quad (3)$$

and

$$P_A+P_B=1 \quad (4)$$

Where ε_A and ε_B are the dielectric functions of the effective medium, material A, and material B respectively, p_A and p_B represent, respectively the packing density of material A and material B. In the field of low absorption, $n^2 >> k^2$ (extinction coefficient) and $\varepsilon = n^2$ (refractive index of Sb_2S_3 deposited at normal incidence), $\varepsilon_A = n_A^2$ (refractive index of Sb_2S_3 deposited at different incident angles) and $\varepsilon_B = n_B^2$ (refractive index of air). Variation of the packing density with the flux incident angle for OAD Sb_2S_3 thin films is shown in Table **1**. As can be seen, the packing density of Sb_2S_3 films decreases with the increase of the incident angle. Indeed, when the incoming flux atoms arrive at the substrate surface normally, the films are compact and the packing density is 1. At α = 85°, the packing density decreases to 0.65 which means that most part of Sb_2S_3 film are filled with air. As a result, the film becomes a mixture of the film material and air at high incident angle. This occurs because atomic shadowing which dominates the growth process of OAD films produces areas that vapor flux cannot directly reach while adatom mobility is too low for surface diffusion to fill the voids. Thus porous and low density thin films are produced [21].

Table 1: Thickness, roughness, refractive index, packing density and band gap values of Sb_2S_3 thin films deposited at different incident angles.

Flux incident angle (°)	Thickness (nm)	Roughness (nm)	Refractive index	Packing density	E_g (eV)
0	830	2.50	2.98	1	1.87
20	740	3.00	2.88	0.94	1.82
40	650	3.50	2.63	0.82	1.88
60	425	6.00	2.55	0.77	1.89
70	260	7.50	2.38	0.70	1.86
85	155	9.50	2.27	0.65	1.88

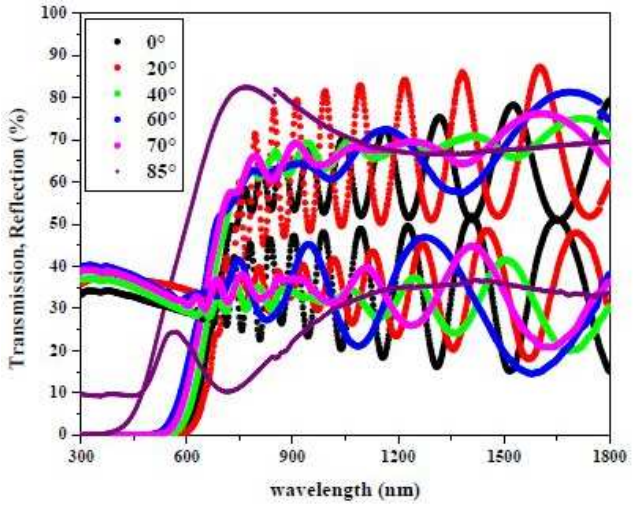

Fig. 4: Transmittance and reflectance spectra of Sb_2S_3 thin films deposited at different incident angles.

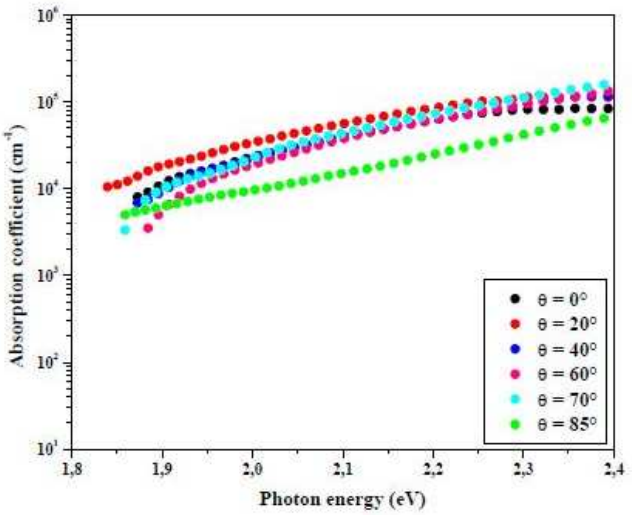

Fig. 5: Absorption coefficient spectra of the Sb_2S_3 thin film deposited at different incident angles.

The optical absorption coefficients were evaluated from the transmittance T(λ) and reflectance R(λ) data using the formula [22]:

$$\alpha = \frac{1}{d}\ln\left(\frac{(1-R)^2}{T}\right) \quad (5)$$

Where α is the absorption coefficient and d is the film thickness. Figure **5** shows the absorption coefficients as a function of the photon energy. It can be seen that all the films of Sb_2S_3 have relatively high absorption coefficient (10^4-10^5 cm^{-1}) in the visible range and near-IR spectral range. This result is very important because we know that the spectral dependence of the absorption coefficient affects the solar cell conversion efficiency for photovoltaic applications [23].

The absorption coefficient α is related to the energy gap E_g according to the equation [24,25]:

$$(\alpha h\nu) = A(h\nu - E_g)^n \quad (6)$$

where A is a constant that depends on the transition probability, h is the Planck constant and n equals 1/2 for direct gap. The band gap E_g was determined by extrapolating the straight line of the $(\alpha h\nu)^2$ versus (hν) curve to intercept the horizontal photon energy axis (figure **6**). All the energy gap values of Sb_2S_3 thin films were assembled in table **1**. As can be seen, all the direct band gap energy values are around 1.87 eV. So, in our case the oblique angle deposition has not a great effect on the energy band gap because the films were globally amorphous as we show by X-ray diffraction measurements.

5 Conclusions

Sb_2S_3 thin films were deposited by thermal evaporation method with oblique angle deposition. All the deposited films were amorphous as confirmed by the X-ray diffraction analysis. The microstructure of Sb_2S_3 thin films was composed of slanted columns at high incident angle. The optical parameters were calculated from the transmission and reflection spectra's of the Sb_2S_3 thin films. It was shown that the refractive index and thickness decreased with increasing of the incident angle and all the films have relatively high absorption coefficients (10^4-10^5 cm^{-1}) in the visible range and near-IR spectral range. The flux incident angle affects the optical properties of Sb_2S_3 thin films. This is very important because the oblique incident angle method can be used to enhance the physical properties of Sb_2S_3 thin films.

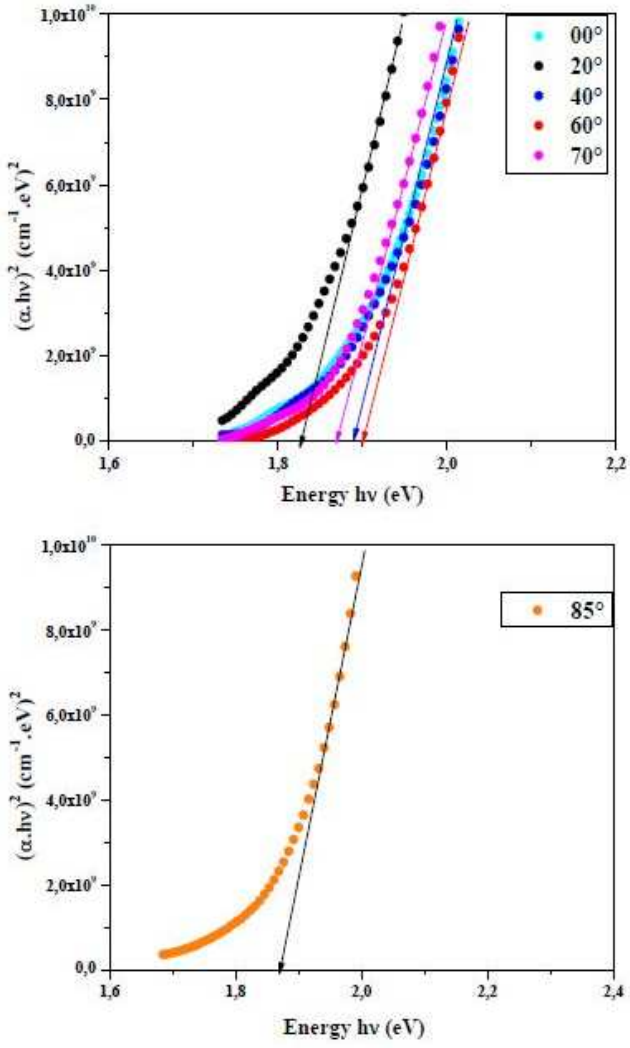

Fig. 6: Optical direct band gap of the Sb_2S_3 thin film deposited respectively at diffrent incident angles.

References

[1] K. Robbie, M.J. Brett, "Sculptured thin films and glancing angle deposition: Growth mechanics and applications," Journal of Vacuum Science and Technology, **15**, 1460 (1997).

[2] J. J. Steele and M. J. Brett, "Nanostructure engineering in porous columnar thin films: recent advances," Journal of Materials Science: Materials in Electronics, **18**, 367 (2007).

[3] J. Lintymer, N. Martin, J.M. Chappe, P. Delobelle, J. Takadoum, "Glancing angle deposition to modify microstructure and properties of sputter deposited chromium thin films," Surface and Coatings Technology, **26**, 180-181 (2004).

[4] Y.-P. He and Y.-P. Zhao,"Advanced multi-component nanostructures designed by dynamic shadowing growth," Nanoscale, **3**, 2361 (2011).

[5] I. Hodgkinson, S. Cloughley, Q. H. Wu, and S. Kassam, "Anisotropic scatter patterns and anomalous birefringence of obliquely deposited cerium oxide films," Applied Optics, **35**, 5563 (1996).

[6] A. G. Dirks and H. J. Leamy, "Columnar microstucture in vapor deposited thin films," Thin Solid Films, **47**, 219 (1977).

[7] R. N. Tait, T. Smy, and M. J. Brett, "Modelling and characterization of columnar growth in evaporated films," Thin Solid Films, **226**, 196 (1993).

[8] G.K. Kiema, M.J Colgan, M.J. Brett, "Dye sensitized solar cells incorporating obliquely deposited titanium oxide layers," Solar Energy Materials and Solar Cells Sol, **85**, 321 (2005).

[9] R. Sharma, A. Ghule, V. Taur, R. Joshi, R. Mane, J.C. Vyas, G. Cai, T. Ganesh, S. Min, W. Lee, S.H. Han, "Growth of nanocrystalline CuIn3Se5 (OVC) thin films by ion exchange reactions at room temperature and their characterization as photo-absorbing layers," Applied Surface Science, **255**, 8158 (2009).

[10] S. Kuze,D. Duboulay, N. Ishizawa, A. Saiki and A. Pring, "X-ray diffraction evidence for a monoclinic form of stibnite, Sb2S3, below 290 K," American Mineralogist, **89**, 1022 (2004).

[11] K. Y. Rajpure, C. H. Bhosale, "Effect of composition on the structural, optical and electrical properties of sprayed Sb2S3 thin films prepared from non-aqueous medium," Journal of Physics and Chemistry of Solids, **61**, 561 (2000).

[12] N. Ghrari, F. Aousgi, M. Zribi, M. Kanzari, "Comparative studies of the properties of thermal annealed Sb2S3 thin films," Chalcogenide Letters 217, (2010).

[13] A.R. Shetty , A. Karimi, M. Cantoni, "Effect of deposition angle on the structure and properties of pulsed-DC magnetron sputtered TiAlN thin films," Thin Solid Films, **519**, 4262 (2011).

[14] D. Vick, L.J. Friedrich, S.K. Dew, M.J. Brett, K. Robbie, M. Steo, T. Smy, "Self-shadowing and surface diffusion effects in obliquely deposited thin films," Thin Solid Films, **339**, 88 (1999).

[15] K. Djessas, G. Masse, M. Ibannaim, ”Diffusion of Cu, In, and Ga in In2Se3/CuGaSe2/SnO2 thin film photovoltaic structures,” Journal of The Electrochemical Society, **147**, 1235 (2000).
[16] A.C.K. Chan, H. Wang, M.J. Chan, Electron Device Letters, **22**, 384 (2001).
[17] J. Poortmans, V. Arkhipov, ”Thin Film Solar Cells: Fabrication, Characterization and Applications,” John Wiley & Sons, New York, 2006.
[18] X. Xiao, G. Dong, C. Xua, H. Hea, H. Qia, Z. Fana, J. Shaoa, ”Structure and optical properties of Nb2O5 sculptured thin films by glancing angle deposition,” Applied Surface Science, **255**, 2192 (2008).
[19] K.L Chopra, Thin film phenomena, Mc Graw-Hill, New York, 721 (1969).
[20] D. Stroud, ”The effective medium approximations: Some recent developments,” Superlattices and Microstructures, **23**, 567 (1998).
[21] D. Vick, L.J. Friedrich, S.K. Dew, M. J. Brett, K. Robbie, M. Steo, T. Smy, ”Self-shadowing and surface diffusion effects in obliquely deposited thin films,” Thin Solid Films, **349**, 88 (1999).
[22] D.E. Milovzorov, A.M. Ali, T. Inokuma, Y. Kurata, ”Optical properties of silicon nanocrystallites in polycrystalline silicon films prepared at low temperature by plasma-enhanced chemical vapor deposition,” Thin Solid Films, **382**, 47 (2001).
[23] I. Konovalov, ”Intermixing, band alignment and charge transport in AgIn5S8/CuI heterojunctions,” Thin Solid Films, **451**, 413 (2004).
[24] J. T. Tauc, Amorphous and Liquid Semiconductors Plenum Press, New York, (1974).
[25] E. A. El-Sayad, ”Compositional dependence of the optical properties of amorphous Sb2Se3-xSx thin films,” Journal of Non-Crystalline Solids, **354**, 3806 (2008).